Performance Analysis of an Integrated PV/T–TEC System with a PID enabled DC–DC Boost Converter for Photovoltaic Thermal Management

Priyo Adi Sesotyo
Department of Electrical Engineering, Semarang University, Semarang, Indonesia

La Ode Muhamad Idris
Department of Electrical Engineering, Semarang University, Semarang, Indonesia

Taufik Dwi Cahyono
Department of Electrical Engineering, Semarang University, Semarang, Indonesia

Ery Sadewa
Department of Electrical Engineering, Semarang University, Semarang, Indonesia

Abstract: The temperature-induced efficiency loss of 0.4% to 0.5% for every °C above 25 °C alongside the inherent variability in solar irradiance, poses a critical challenge to the efficiency and stability of Photovoltaic (PV) modules. This study addresses this limitation by developing and analyzing an Integrated Photovoltaic Thermal-Thermoelectric Cooler (PV/T–TEC) system designed for robust thermal management and enhanced energy yield. The proposed system utilizes a synergistic hybrid cooling mechanism: a passive PV/T air collector for bulk heat dissipation from the PV panel's rear surface, coupled with an active Thermoelectric Cooler (TEC) for precise temperature stabilization. The electrical energy flow is managed by a DC–DC Boost Converter employing a PID controller, with a focus on input disturbance rejection, ensuring the TEC operates at an optimal, stable power point.Simulation and performance analysis demonstrate the significant advantages of this hybridized approach. The PV/T air collector was confirmed as the primary thermal component, achieving a peak heat dissipation Q_{Emit} approximately 7.5 times greater than the TEC-only configuration. This strategic pre-cooling successfully stabilizes the TEC's hot-side temperature, enabling the TEC to operate with a low operational temperature differential ΔT and resulting in an exceptionally high calculated Effective System

Correspondents Author:
Priyo Adi Sesotyo, Department of Electrical Engineering, Universitas Semarang, Indonesia
Email: psesotyo@usm.ac.id

Received November 19 2025; Revised December 14, 2025; Accepted December 15, 2025; Published December 15, 2025.

Coefficient of Performance COP peaking at 14.5. The system maintains a stable operating point during peak solar radiation, maximizing the Net Electrical Power Gain. In conclusion, the integration of passive PV/T cooling, active TEC cooling, and a PID-enabled DC–DC Boost Converter provides an exceptionally efficient and stable solution for PV thermal management. The research strongly supports the efficacy of this hybrid system for significantly improving the overall energy efficiency and sustainability of solar energy applications.

Keywords: Coefficient of Performance (COP), DC-DC Boost Converter, PID Control, Photovoltaic Thermal (PV/T), Thermoelectric Cooler (TEC)

Introduction

The rapid growth in global energy demand, driven by industrialization, population growth, and technological advancements, has intensified the need for sustainable, renewable energy solutions. Among renewable resources, solar energy stands out as one of the most abundant and promising alternatives due to its universal availability and environmental compatibility. The photovoltaic (PV) technology, which directly converts solar radiation into electricity, has gained remarkable attention as a clean energy source for residential, commercial, and industrial applications. However, the conversion efficiency of conventional PV modules is inherently limited, typically ranging from 15% to 22% for commercial silicon-based cells—owing to material constraints and environmental factors such as solar irradiance and temperature variations (Kalogirou, 2009; Singh & Ravindra, 2012). The efficiency of a PV device is negatively impacted as its power output gradually diminishes over time. The decline is due to exposure to solar radiation, improper installation, inadequate maintenance, and various external factors (Balasaheb et al., 2018).

Apart from the gradual decline, the efficiency of a PV cell can be influenced by (i) reflection. Reduced light can be reduced by applying an anti-reflection coating and utilizing a textured glass surface. The excess heat generated by photon absorption is unavoidable. Upon the impact of solar rays on the photovoltaic cell surface, a fraction of absorbed photons transform their energy into heat, while the remaining photons facilitate the displacement of electrons from their atomic bonds, leading to the creation of charge carriers and the flow of electric current through the p-n junction. (iii) The elevated temperature. Solar photovoltaic systems perform optimally in colder temperatures. Increased temperatures result from low humidity, solar radiation reflected to Earth, and the surplus heat absorbed by the solar PV surface. Increased temperatures shift the properties of the p-n junction, leading to a marginal increase

in current flow, whereas a considerably more pronounced decrease in voltage will affect the generation of electrical power. Enhancing thermal management can potentially improve the efficiency and lifespan of solar photovoltaic systems. One of the primary challenges affecting PV performance is the temperature rise. As the operating temperature of PV cells increases, the open-circuit Voltage decreases while the current marginally increases, resulting in a net reduction in power output. The efficiency of most crystalline silicon PV modules typically drops by 0.4%–0.5% per °C above the standard test condition (STC) temperature of 25°C (Adeeb et al., 2019). This temperature-induced degradation not only reduces energy yield but also shortens the lifespan of PV modules.

According to Narkwatchara et al., the tropical climate region adversely affects the electrical output of PV collectors (Narkwatchara et al., 2020). Additionally, Misha et al. conducted simulations and experimental evaluations of the PV/T water system under Malaysian climatic conditions. The findings indicated a reduction in cell temperature with an elevated mass flow rate. The maximum electrical efficiency has been determined to be 11.71% (Misha et al., 2020). The operational temperature of the PV collector can be reduced by integrating the PV panel with a thermal collector, creating a PV/T collector that absorbs the unused waste heat.

Superior electrical efficiency in water-based PV/T systems, relative to their air-based counterparts, underscores the fundamental efficiency of the hybrid system, which is contingent upon the heat transfer medium (Kazem, 2019). The DC-DC boost converter maintains and regulates this essential electrical output advantage, ensuring the voltage is at the intended level and optimizing power extraction using MPPT (Esram & Chapman, 2007). Advancements in system performance are achieved through the application of thermoelectric cooling (TEC), and a design strategy focused on decreasing TEC cooling power enhances the Coefficient of Performance (COP), utilizing the modular nature of these devices to establish an integrated, highly efficient hybrid system (Dehra, 2018). Therefore, maintaining optimal cell temperature is essential to maximize electrical performance and ensure long-term system reliability.

Research Gap and Motivation

Several studies have explored similar hybrid PV/T and PV/TEC configurations, as found in Table 1, categorize into three (3) distinctive purposes : (1) Hybrid System Benefits and Configuration. Hybrid PV/T systems offer multiple benefits beyond simple electrical generation, primarily by utilizing thermal cooling to boost electrical efficiency while simultaneously producing usable heat. For instance, a water-based PV/T system can generate an average power up to 6% higher than a conventional PV panel while also producing warm

water for further applications (Kazem, 2019). To further enhance electrical performance, many studies have integrated Thermoelectric Coolers (TECs) directly with the PV module. This TEC-assisted configuration has been shown to maintain a temperature reduction of up to 12◦C, translating to a significant 6–8% increase in electrical efficiency under high irradiance conditions (Ali Taher & Al-Hamadani, 2024). Crucially, the practical adoption of the base PV/T system is favored by its straightforward installation and minimal initial and maintenance expenses (Talal et al., 2024). (2) Power Management and Control. Optimizing the performance of these hybrid systems requires sophisticated power conditioning and control circuitry. A crucial element is the DC-DC boost converter, which, when integrated with the TEC and PV system, allows for the dynamic management of power balance. This ensures adequate current is supplied to the TEC for necessary temperature control without significantly compromising the net electrical efficiency (Sesotyo et al., 2025). Furthermore, a proper power conditioning circuitry must include a Maximum Power Point Tracker (MPPT) to ensure the optimal flow of energy between the PV/TEC components and the load (Twaha et al., 2017). Implementing such control, as shown in one study, involved integrating a DC-DC Converter and TEC with an MPPT controller and battery, using an adaptive duty cycle to maintain voltage matching and optimize the Maximum Power Point (MPP) (Toumi et al., 2021). (3) Cooling Media and Advanced Enhancements. The choice of cooling medium and the use of additional materials can significantly affect the system's overall gain. While water-based cooling is highly effective, coupling a PV/TEC installation with a Thermal Interface Material (TIM) can provide modest but measurable gains, reporting an electrical efficiency increase of 1.1% when the TEC heatsink is cooled by water (Kotkondawar et al., 2021). Some studies have focused on using Thermoelectric Generators (TEG) to power the TEC with wasted heat, concluding that this PV/T with passive cooling by a TEG-powered TEC can increase the overall PV system efficiency by 15.5% (Faheem et al., 2024). For advanced performance, coupling PV/T with nanofluid as a cooling medium and intelligent control circuits, along with additional wind velocity, has been confirmed to enhance total exergy efficiency (Wu et al., 2015). Even simpler methods, like using air flow as a cooling fluid for PV/T and TEC covering 12% of the back surface, can still yield an electrical power gain of 0.3% (Amrizal et al., 2022). Overall system performance can be dramatically improved through optimized integration, such as an integrated PV/T–TEC model with an opaque PV backsurface and an air duct, showing an overall exergy gain reaching up to 100% (Dimri et al., 2018).

Tabel 1 Research Gap

Author	Thermal Collector	Air	Water	Nano fluid	DC-DC Converter	Inter face	Control ler	TEG	TEC
(Twaha et al., 2017)	☑				☑		☑	☑	
(Kazem, 2019)	☑		☑						
(Ali Taher & Al-Hamadani, 2024)					☑				☑
(Sesotyo et al., 2025)					☑		☑		☑
(Kotkondawar et al., 2021)						☑			☑
(Toumi et al., 2021)					☑		☑		☑
(Faheem et al., 2024)	☑	☑						☑	☑
(Wu et al., 2015)	☑			☑					
(Amrizal et al., 2022)	☑	☑							☑
(Talal et al., 2024)	☑	☑	☑						
(Dimri et al., 2018)	☑	☑							☑

Therefore, this study aims to develop and analyze an integrated Photovoltaic Thermal (PV/T) and DC-DC Boost Converter–Thermoelectric Cooler (TEC) model for photovoltaic energy performance optimization. The system is modelled and simulated using MATLAB/Simulink to evaluate the coupled electrical–thermal interactions and assess the benefits of active temperature control and power management. Specifically, this research seeks to:

1. Investigate the impact of TEC-assisted cooling on the electrical efficiency and temperature regulation of PV systems.
2. Examine the role of the DC-DC boost converter in maintaining optimal voltage levels and energy balance within the integrated system.
3. Evaluate the overall heat removal improvement of the hybrid PV/T–TEC configuration under dynamic irradiance and temperature conditions.

This hybrid approach leverages both passive thermal extraction from the PV/T system and active thermoelectric cooling, both regulated by power electronics embedded with a PID controller for optimal energy conversion. The expected outcome of this work is to provide a comprehensive modelling framework that demonstrates the potential of combining thermal energy recovery, active cooling, and power electronic regulation to enhance the efficiency and sustainability of solar energy systems. The findings may serve as a foundation for future experimental studies and practical implementations of smart hybrid PV systems capable of real-time optimization in diverse environmental settings.

Research Method

The operational characteristics of a solar PV module can be ascertained via the key parameters documented in Table 2, which details the Solar PV Parameters for 100 Wp, sourced from , encompassing peak power (Pmax), open-circuit voltage (Voc), short-circuit current (Isc), and the maximum power point (MPP), Peak power is the maximum electrical power the module delivers under standard test conditions and reflects its maximum energy output. Open-circuit voltage is the voltage measured at the module's terminals when no current is flowing, indicating the module's maximum voltage. The short-circuit current, produced by directly connecting the module's terminals, represents the maximum current output under ideal conditions. Maximum power point is the voltage and current configuration that results in the module's highest power output.

Table 2 Solar PV Parameters

Parameters (STC = Standard Test Conditions), where as at irradiance of 1000 W/m², ambient temperature of 25 °C and an air mass of 1.5	**Unit**	**Value**
Pmax (Peak Power)	Wp	100
V_{oc} (Voltage Open Circuit)	V	115.8
I_{sc} (Current Short Circuit)	A	1.27
V_{mpp} (Voltage Maximum Power)	V	94.4
I_{mpp} (Current Maximum Power)	A	1.06
Number of Series	Pcs	1
Number of Parallel	Pcs	1
Dimension (A)	m²	1

This PV module is designed to operate at a relatively high voltage (around 94.4 V at peak power) while delivering a moderate current, making it suitable for applications with power conditioning circuitry, such as a DC-DC boost converter. The parameters of the PV module, specifically Vmpp and Impp, are critically important for the operation of the DC-DC converter, as it performs MPPT. The Impp of 1.06 A and Vmpp of 94.4 V, in conjunction with a DC-DC boost converter, define the power that the Solar PV can deliver. The mechanism that ensures the system actually operates at these optimal values under all conditions is a practical choice, especially in a PV/T system.

The Voltage supplied to the TEC is derived from the Solar PV output; its instability is contingent on daily irradiance. Variations in solar irradiance cause fluctuations in the photovoltaic panel's electrical output, which directly impacts the thermoelectric cooler's power supply. A compromised or fluctuating power supply could impair cooling performance or cause intermittent thermoelectric cooler operation.

Increased irradiance leads to higher PV panel temperatures due to a greater heat absorption. Solar PV performance changes drastically under actual operating conditions, as reported (Amelia et al., 2016). As the solar irradiance decreases from 1000 W/m2 to 200 W/m2, the maximum power point drops sharply, reducing the peak output from 66.6 W to 17.4 W. The power drops because fewer photons strike the cell, directly decreasing the generated current (Impp) and, therefore, the power. Conversely, the cell temperature has an inverse effect on performance at an irradiance of 1000 W/m2; at a high cell temperature of 89 °C, the maximum power output is only 66.6 W, which is considerably less than the 100 Wp rating at 25 °C, as indicated in the STC table. An increase in cell temperature leads to a decrease in the open-circuit voltage (Voc) and maximum power point voltage (Vmpp), thus reducing the overall electrical power output. Therefore, the DC-DC converter's MPPT circuit must continuously track the maximum power point, which shifts with fluctuations in irradiance (primarily affecting current) and cell temperature (primarily affecting voltage), as indicated by the various peaks on the P-V curve, which can lead to thermal inefficiencies, potentially diminishing the photovoltaic (PV) module's performance.

Perfecting the thermal management of photovoltaic (PV) cells is critical for greater output. Heat is transferred through a solid via conduction. The PV/T system's solar energy conversion process is subject to the First Law of Thermodynamics (Energy Conservation). Q_{source} (Source Heat) where the heat is that needs to be removed in a solar thermal system, or is considered a loss (waste heat) in a PV system. $P_{absorbed}$ as the total solar power absorbed by the device, where A is the entire collector area, and G is the global solar irradiance (or insolation) incident on the collector surface (W/m²). τ_G (Transmittance of Glass/Glazing), the transmittance of the glass cover or glazing material is the fraction of incident solar radiation that passes through the glass to reach the absorber plate or PV cell, and it ranges from 0 to 1. α_C (Absorptance of Collector) active surface (absorber plate or solar cell), that represents the fraction of the radiation that reaches the surface, which is actually absorbed (not reflected), where the value is between 0 and 1, as presented in Table 3.

Table 3 PV/T Parameters

Parameters	Unit	Value
Glass Transmittance (τ_G)	dimensionless	0.90
Cell Absorptance (α_C)	dimensionless	0.96

The Glass Transmittance ($\tau_G = 0.90$) indicates that 90% of the incident solar radiation passes through the PV module's glass cover to reach the cells. Subsequently, the Cell Absorptance ($\alpha_C = 0.96$) indicates that 96% of the radiation reaching the cells is absorbed by them. These parameters are

essential inputs for calculating the total energy absorbed by the PV cells. Since only a fraction of this absorbed energy is converted into electrical power (as indicated by the P-V curve), the large remainder must be calculated as waste heat, which is the energy targeted for removal by the PV/T system (air flow in the duct) to both increase the system's total thermal output and prevent detrimental cell temperature rise.

P_{elec} (Electrical Power) represents the electrical power output generated by the device (W).

$$P_{absorbed} = A * G * \tau_G * \alpha_C \quad (1)$$

$$P_{elec} = V_{out} * I_{out} \quad (2)$$

$$Q_{source} = P_{absorbed} - P_{elec} \quad (3)$$

A is the total solar power incident on a unit area. Increased temperatures are associated with reduced power output from PV cells. The process of heat conduction, as defined by the heat equation, moves from areas of higher to lower temperature, as specified below:

$$q_x = -kA\frac{dT}{dx} \quad (4)$$

Where: q_x represents heat flux (watts) and k represents thermal conductivity (W/m/^{o}C). Employing the Fourier equation, the heat flow (Q) is given by the formulation

$$Q_{out} = k * A * \frac{(T_H - T_C)}{L} \quad (5)$$

Where: A denotes area (m^2), T_H and T_C represent the hot and cold temperatures (^{o}C), respectively, and L represents length (m), where the bottom PV temperature (T_H) and ambient temperature (T_C) within a day, can be found in the Table 4 below, sourced from Sesotyo et al. (Sesotyo et al., 2022), which illustrates the direct and strong relationship between solar irradiance and the resulting PV module temperature, differentiating between the front (TH) and back (TC) surface measurements.

Table 4 Irradiance & Temperature in the PV Panel

Time	Irr (W/m^2) (G)	T_H (^{o}C)	T_C (^{o}C)
08.00	525.7	47.5	34.8
09.00	777	47.6	34.7
10.00	944.5	43.9	34
11.00	830.5	47.9	35.7
12.00	765.8	47.5	38.3
13.00	609.8	44.4	37.5
14.00	439.5	38.9	36.8
15.00	276.5	35	34.8
16.00	288	35.2	33.8

As the Irradiance (G) increases, both the front surface temperature (TH) and the back surface temperature (TC) also rise. The PV panel's temperature is critically dependent on solar irradiance, as only 10–20% of the incident solar energy is converted to electricity, with the rest being converted to heat, raising the module's temperature. Crucially, the data in Table 4, reveals a significant temperature difference between the front and back surfaces of the PV panel under load, which is essential for systems employing active cooling or thermoelectric devices. Throughout the measurement period (08:00 to 16:00), the front surface temperature (TH) is consistently higher than the back surface temperature (TC), often by several degrees (e.g., 47.5 °C vs. 34.8 °C at 08.00). This thermal gradient is a result of the PV panel's material structure, its thermal transfer processes (conduction, convection, and radiation), and the direct absorption of solar radiation on the front surface. This difference is particularly relevant in hybrid PV/T-TEC systems, where thermal management often focuses on the back surface to extract heat, thereby cooling the cells and mitigating the temperature-induced electrical efficiency losses shown in the P-V curve.

These three synchronized signals (Irradiance, TH, and TC) in the tabel 4, are crucial for the Simulink the Signal Builder model graph, which effectively visualizes the dynamic relationship between solar irradiance and PV panel temperatures over a typical day (8:00 to 16:00). Utilizing the data from Table 4 as input for a Simulink Signal Builder model simulation enables accurate modeling of the PV module's electrical output, as well as the performance of integrated thermal management systems such as Thermoelectric Coolers (TECs) or DC-DC converters, throughout the day.

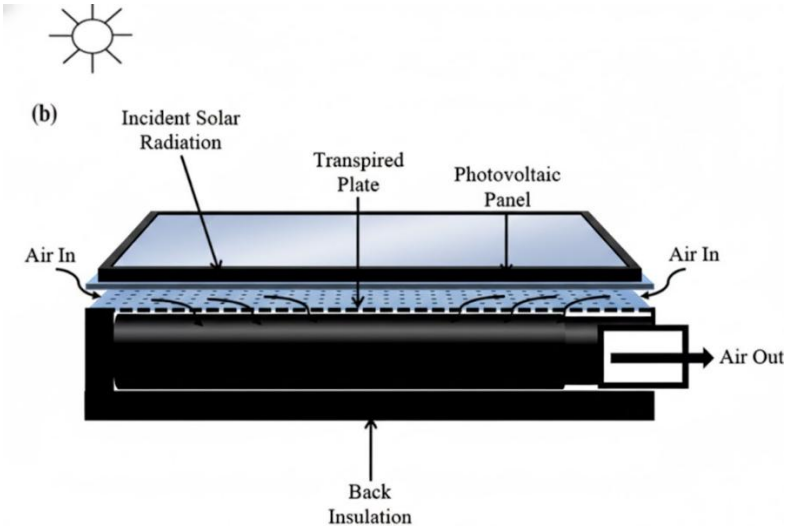

Figure 1 PV/T flat transpired collector with air as the heat exchanger fluid.

Using a photovoltaic panel and a transpired plate permits the system to offset electrical energy use by losing some thermal energy. As can be seen in Figure 1, sourced from (Gholampour & Ameri, 2016), in PV/Thermal flat transpired collector, first, the air flowing between the PV panel and transpired plate captures the heat from the back of PV panel and front of the transpired plate, afterwards, the air captures the heat from the holes and the back of the transpired plate when it is drawn through the holes. The primary purpose of this airflow is passive cooling of the PV panel, which helps maintain lower cell temperatures and thus preserves the module's electrical efficiency. At the same time, the resulting heated air can be collected for space heating or other thermal applications, demonstrating the dual functionality of a PV/T system. Altering the airflow path and adopting porous materials, thin metallic sheets, or fins allowed substantially increasing the thermal and electrical performance of PVT air collectors (Togun et al., 2025).

Despite the enhanced thermal and electrical energy-harvesting potential of the combined PV/T collector, the PV module remains susceptible to elevated operating temperatures due to solar absorption and heat accumulation in the air channel. The electrical efficiency of a photovoltaic cell declines with increasing temperature. Consequently, an extra cooling mechanism is vital to keep the PV module at its ideal operating temperature. Active cooling, such as that provided by a thermoelectric cooler (TEC), helps to eliminate excess heat from the PV surface, thus increasing module electrical output and system efficiency.

The TEC's proposed power supply, derived from a solar PV system, exhibits instability in DC voltage and current, necessitating stabilization via a DC-DC converter. Thermal transfer compound affixes the TEC to the rear of the PV module, facilitating contact of its cold side with the PV module. Based on Figure 2, adapted from (Mooko & Kusakana, 2018) and incorporating a thermal collector, a heat sink, and a thermal transfer compound, the system dissipates heat from the hot side of the TEC into the environment.

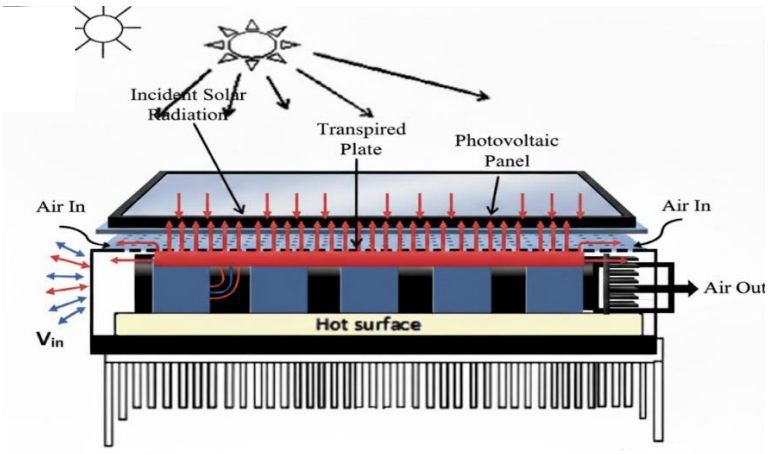

Figure 2 Solar PV Cooling using a TEC

Incident solar radiation strikes the Photovoltaic Panel, which is thermally coupled to the Cold Surface of a series of Thermoelectric Cooler (TEC) modules. The TECs, powered by an external voltage source (Vin), actively pump heat from the cold side (the back of the PV panel) to the Hot Surface, which is connected to a heat-dissipation mechanism, such as a Heatsink with fins. Air is channeled over the TEC's hot side and out, indicating a forced or natural convection method for removing the combined heat (waste heat from the PV panel and heat generated by the TEC). This configuration aims to achieve a high net electrical power output by generating electricity and actively controlling the PV cell temperature, mitigating the significant power losses that occur at high operating temperatures, as shown in the P-V curves.

The thermal equilibrium equations for steady-state conditions are presented, including Peltier heat, conduction losses, and Joule losses (Tsai & Lin, 2010). The following calculates the temperature of PV panels:

$$T_p = \frac{Q_{in} - Q_{out}}{m * c_{pp}} \tag{6}$$

Where T_p is the mean temperature of the PV panel, Q_{in} is the heat input to the PV panel, Q_{out} is the heat output of the panel, m the mass of the panel, and c_{pp} is the average specific heat of the panel. The panel receives its thermal energy input from incident solar radiation. A fraction of the incident radiation is photoelectrically converted; however, the resultant energy increase is predominantly manifested as sensible heat, causing a temperature elevation within the panel, which can be expressed as:

$$Q_{in} = GA * (1 - \in) \tag{7}$$

Here, G symbolizes the incident solar irradiance on the panel's surface, A represents the panel's surface area, and ∈ signifies the panel's electrical conversion efficiency. The formula Q = m*c*ΔT determines the heat extraction. Thermodynamic and heat transfer principles serve as the basis for this equation.

The heat removal factor (FR) quantifies the efficiency of energy collection, defined as the ratio of actual energy gain to the theoretical maximum, based on a fixed collector surface temperature at the fluid's entry. The accuracy of heat removal effectiveness quantification depends significantly on this parameter. The rate of heat removal is mathematically correlated with fluid properties, the collector surface, and FR, with conduction, convection, and radiation playing key roles in heat removal (Abdel-Khalik, 1976).

$$FR = \dot{m} * c_p * A_c * U * \left[1 - e^{\frac{-A_c * U * F'}{\dot{m} * c_p}}\right] \tag{8}$$

Where $\dot{m}$ is the mass flow rate of the cooling fluid, c_p is the specific heat capacity of the cooling fluid (J/kg.K), A_c is the area of the plate (m²), U is the heat transfer coefficient (W/(m².K), F' is the plate efficiency factor, and e is the base of the natural logarithm.

The Peltier module's efficiency is quantified by the COP, which is calculated as follows:

$$COP = \frac{Q_E}{P_{in}} \tag{9}$$

Maintaining the TEC's hot-side temperature (TH) is crucial for maintaining a consistent heat flux (QR) in Watts, which is required to generate the cooling effect (Bayendang et al., 2021). The heat removal Q_R by TEC can be calculated by :

$$Q_R = (SM * T_H * I) - (0.5 * I^2 * RM) - (KM * \Delta T) \tag{10}$$

Where SM is the Peltier coefficient (V), T_C is the cold side temperature (°C), I is the electric current (A), RM is the internal resistance of the Peltier module (Ω), KM is the internal thermal conductivity of the Peltier module (S/m) and ΔT is the delta temperature of hot and cold sides (°C).

Since the Peltier module require the input powered (P_{in}), then

$$P_{in} = V_{in} * I \tag{11}$$

$$V_{in} = (SM * \Delta T) + (I * RM) \tag{12}$$

Where V_{in} is the input voltage to the Peltier module (V).

While the heat rejected (emitted) Q_E by the module, calculated by

$$Q_E = P_{in} + Q_R \tag{13}$$

The heat and power equations are calculated as follows:

The heat of the removal side is,

$$Q_R = -Q_H = -[(SM * T_H * I) + (KM * (T_C - T_H)) + (0.5 * I^2 * RM)] \tag{14}$$

The heat of the emitting side is,

$$Q_E = -Q_C = -[(SM * T_C * I) + (KM * (T_C - T_H)) - (0.5 * I^2 * RM)] \tag{15}$$

And the power consumed by the TEC is,

$$P = Q_R - Q_E = Q_C - Q_H = -[SM * I * (T_H - T_C) + I^2 * RM] \tag{16}$$

The operational effectiveness of a TEC module is fundamentally defined by three critical metrics: the Seebeck coefficient, electrical resistance, and thermal conductance. The Seebeck coefficient is a measure of the Voltage generated per unit temperature difference across the thermoelectric materials of the module, indicating the efficiency of converting thermal gradients into electrical energy. The degree to which the module opposes the flow of electric current is reflected in its electrical resistance. The thermal conductance, in conclusion,

quantifies the ease with which heat traverses the TEC module by conduction from the hot to the cold side.

Various temperature-differential stages, when available, affect the TEC's COP, sourced from Laird Thermal System, (Laird Thermal Systems, 2022). With an increase in the maximum temperature difference (ΔT) requested from the thermoelectric cooler (TEC), when the PV panel temperature is cooled to a significantly lower level, the COP experiences a sharp decline, eventually approaching zero, attributed to substantial power consumption relative to minimal cooling. To achieve acceptable COP results for the TEC, the temperature difference (ΔT) must be limited to ensure that the electrical power consumed by the TEC (Pin) remains below the electrical power generated by the PV panel.

This means that a single stage of temperature differential results in a lower temperature difference and a higher COP. Lowering thermal conductance helps sustain a larger temperature differential by reducing undesirable heat transfer, thereby boosting cooling performance. The parameters presented in Table 5, sourced (Sesotyo et al., 2025), provides the critical constants required to model the thermal and electrical performance of the Thermoelectric Cooler (TEC) within a Simulink simulation of the hybrid PV/TEC system, are directly inserted into the Simulink model's equations for the TEC block to accurately simulate its cooling power (Qc) and power consumption (Pin) under varying thermal loads from the PV panel and electrical control from the DC-DC converter. These parameters define how the TEC converts electrical power into a temperature difference and heat transfer.

Table 5 TEC Parameters

Parameters	Unit	Value
Seebeck Coefficient (SM)	V/K	$220*10^{-6}$
Electrical Resistance (RM)	Ohm	0.005
Thermal Conductance (TM)	W/K	$1.5*10^{-3}$

The incorporation of Solar PV and TEC is illustrated in Figure 3, sourced from Sesotyo, et al. (Sesotyo et al., 2025), with details of the calculations and simulations of all parameters from the TEC and Solar PV systems.

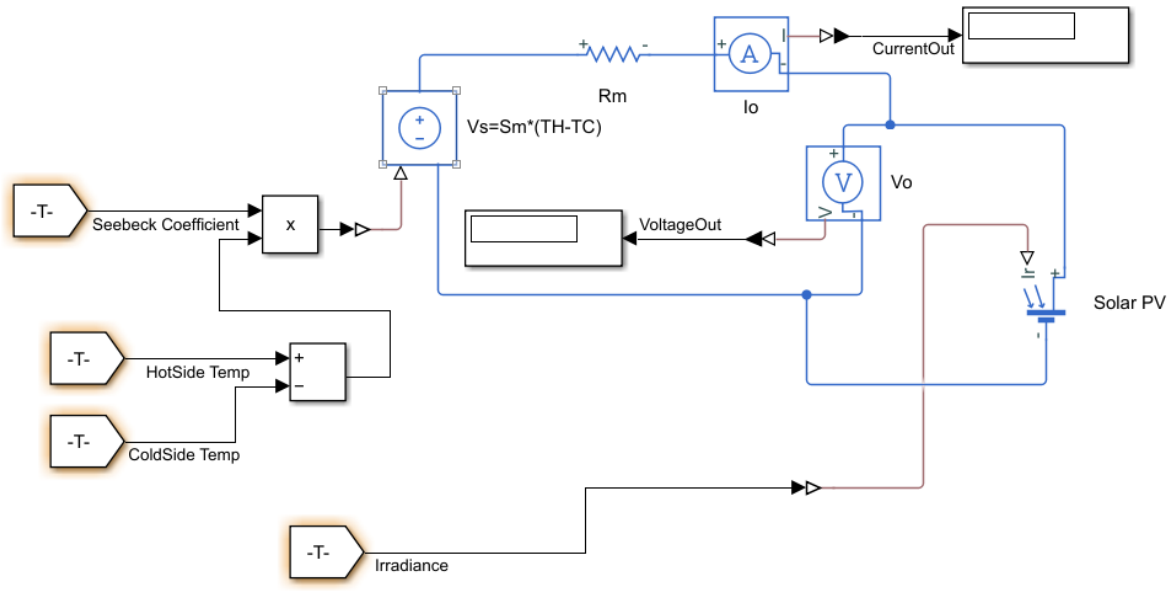

Figure 3 Equivalent circuit of the integrated PV & TEC module for -I and +V

A DC-DC converter comprises two primary elements: the circuitry and the regulatory/control mechanism (Dokić & Blanuša, 2015). The DC-DC converter's elements are displayed in Fig. 4 and include an inductor, a capacitor, a diode, and a switch. Switch-mode power supplies, electric vehicles, electric motor drives, electric braking systems, and solar- and wind-based microgrids extensively use DC-DC converters (Momoh, 2018). The essential structure of the power converter topology necessitates a minimum quantity of electrical components. This power converter was chosen for this research primarily because of its operational versatility and structural elegance.

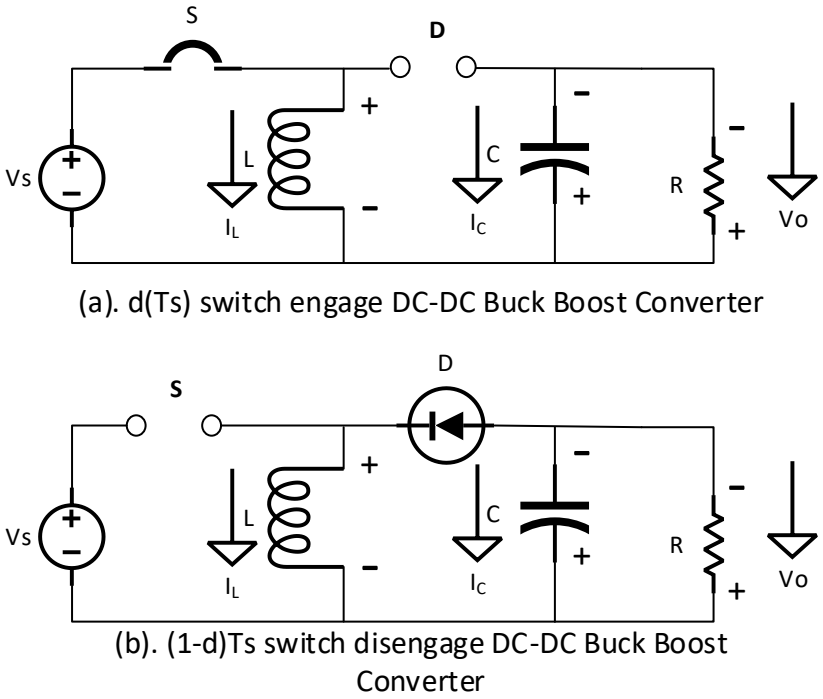

Figure 5 DC-DC Buck-Boost Converter in operational states

Figure 5, sourced (Molina-Santana et al., 2023) and (Bhattacharjee & Saharia, 2014), schematically depicts the various operating states of the power converter. These are used to construct a model of the ideal power converter. The circuit shown in Fig. 5(a) is valid during the converter's on-state, whereas Fig. 5(b) governs the off-state. Each switching time (Ts) causes two operational modes. The primary switch remains engaged for a duration of (dTs) during the initial operational phase, subsequently transitioning to the disengaged state for a period of (1-d) Ts.

Through the use of a single switch operating at a 0.5 duty cycle, the circuit generates a negative output voltage under conditions of negative input voltage. The output voltage is stabilized by this component, which utilizes a step-up or step-down converter to counteract fluctuations in the input voltage. Changes in load and line voltage impact the average load current. Changes in solar irradiance considerably affect the Voltage produced by photovoltaic systems. Buck-boost converters are capable of regulating the system output to the intended level.

$$V_o = V_s * \frac{D}{(1-D)} \tag{17}$$

$$D = \frac{V_o}{V_o - V_s} \tag{18}$$

$$L = \frac{V_s * D}{F * \Delta L} \tag{19}$$

Where L represents the inductor, Vs signifies the input voltage, D denotes the Duty Cycle, F indicates the switching frequency, and ΔL is the inductor current ripple value.

The buck-boost converter ensures output voltage stability regardless of input voltage variations. DC-DC buck-boost converters are capable of transforming input voltages of different polarities and magnitudes into a stable output voltage. The value of these across different power electronics sectors is significant, particularly in the realm of renewable energy systems. There is a need to improve the control method. The research employs a PID (Proportional, Integral, Derivative) control algorithm.

PID controllers combine proportional, integral, and derivative control strategies. During operation, the standard PID parameters generally stay consistent, which may result in controller failure when unpredicted disturbances or environmental fluctuations arise.

Boost DC-DC converters use pulse-width modulation. Researchers have used various controllers with pulse-width modulation methods, where PID control elements constitute the dynamic compensator (Qadir & Ati, 2024), a common feature of nearly all PWM DC-DC controllers, as depicted in the Figure. 7, sourced from (Pratama Putra et al., 2023). The system's nonlinearity results in a deviation from the traditionally accepted linear-invariant PID control structure. Within a buck-boost control system using PWM and a time-dependent duty cycle, variations in the output inductance and capacitance occur. The buck-and-boost inductors add to a non-standard proportional-integral component.

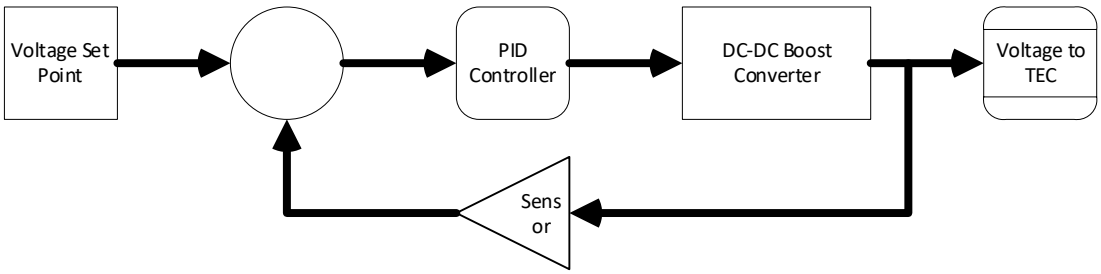

Figure 7 PID Controller implemented on DC-DC Buck-Boost Converter

Industrial control systems commonly integrate PID controllers into their architecture. The system's strengths encompass diminished maintenance requirements and augmented stability. Optimal functionality is achieved through the integration of proportional, integral, and derivative control mechanisms. Their ease of implementation and simplicity allow for their application in various fields. A broad spectrum of industrial applications, including

electrical, thermal, and mechanical engineering, utilize Proportional-Integral-Derivative (PID) controllers. Accurate adjustment of PID parameters as found in Table 6, sourced (Sesotyo et al., 2025) is paramount for ensuring maximum performance and stability. Equalizer settings require optimization for consistent functionality of the plant system. Enhancements to control system output behavior can be achieved through diverse tuning methodologies, including manual and automated approaches (Pathiran, 2019).

Table 6 PID Parameters

Parameters	Value
Proportional (P)	4.795
Integral (I)	47.953
Derivative (D)	0

As illustrated in the figure 8. The two scenarios depict dissimilar methodologies for modeling a hybrid solar system that uses a TEC for thermal management, commencing with identical environmental inputs. Scenario 1 simulates a rudimentary PV system incorporating active cooling via a TEC, whereas Scenario 2 simulates a more intricate system integrating a PV/T collector with a TEC that utilizes passive / thermal pre-cooling before active cooling. Scenario 2's objective is to assess how incorporating PV/T thermal cooling can enhance the TEC's overall cooling efficiency, potentially reducing power consumption and optimizing the system's net electrical efficiency.

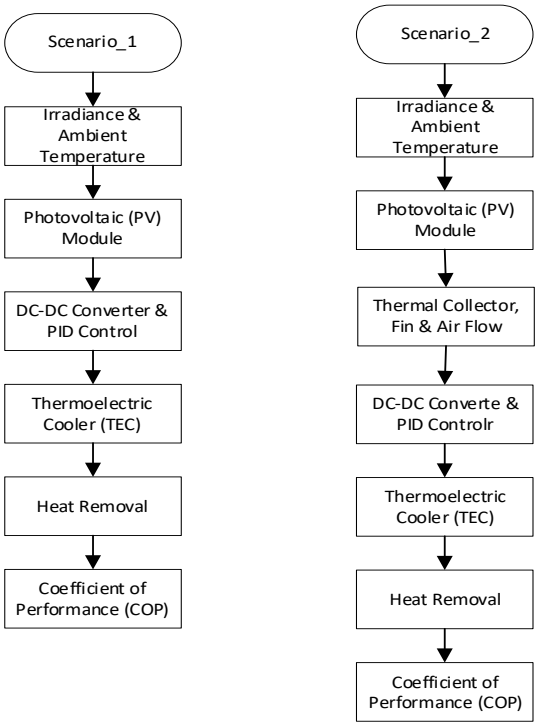

Figure 8 Scenario 1 and 2 flow chart

The proposed model is shown in Fig. 9. The duty cycle (D) is expected to vary with the output voltage, and validation by (Corapsiz & Kahveci, 2019) confirms that when D < 0.5, the output voltage is less than the input voltage. The model illustrated in Fig. 8 is further supported by the research of (Soheli et al., 2018), which shows an increase in voltage gain with increasing D.

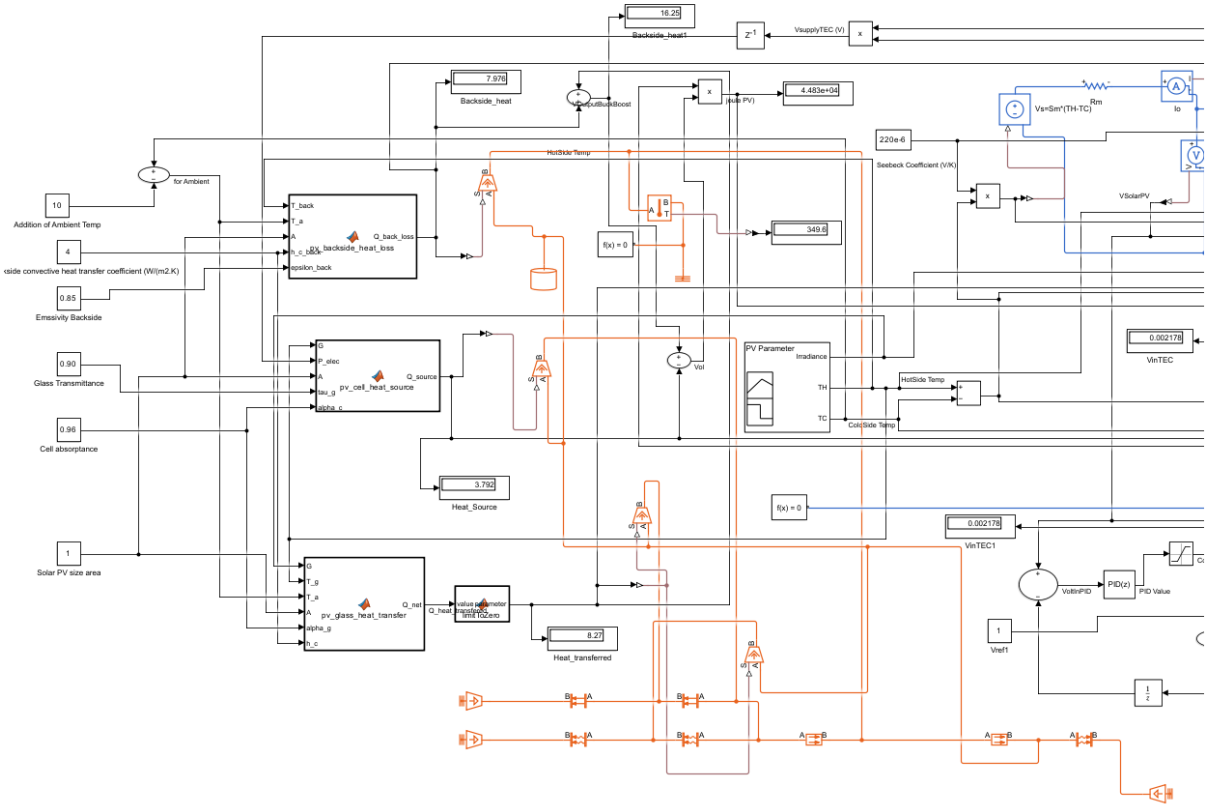

Figure 9 Q Source with radiative heat, conductive and convective heat

Simulation significantly benefits prototype development by enabling cost-effective, efficient design, development, and testing. The simulation platform provides an ideal setting for evaluating the performance of the designed PID controller. Using closed-loop control in PV-powered TEC systems introduces a feedback mechanism to govern the TEC's cooling output, thereby improving stability, efficiency, and adaptability to fluctuating solar irradiance. A closed-loop control system that dynamically adjusts the TEC module's power supply to meet cooling requirements continuously monitored system parameters, including temperature, current, and Voltage (Pathiran, 2019).

The analysis, which involved experiments and simulations, focused solely on an integrated PV/T system that utilized a 100 Wp monocrystalline PV module coupled with a passive metal-fin heat sink. Thermal management is solely accomplished by a single TEC module that is powered by the PV/T output through a DC-DC Boost Converter, incorporating PID control.

The research is restricted due to the system's design, which does not include a battery, nor a Solar Charge Controller.

Result and Discussion

Unlike prior studies, this research uses variable irradiance for more realistic simulations. Real-world PV system behaviour is modeled using simulated changes in solar irradiance. These variations affect solar PV output voltage and current. These scenarios enable accurate PV system assessment and optimization.

Scenario 1: PV-TEC with DC-DC Buck-Boost equipped with PID controller and Input disturbance rejection focused tuning.

A PV system integrated with a TEC and a DC-DC buck-boost converter, incorporating a PID controller with input disturbance-rejection-focused tuning, is modeled to achieve high-performance, energy-efficient temperature control. The system effectively mitigates real-world challenges, including variations in solar irradiance (input disturbances), thereby ensuring stable power delivery to the TEC irrespective of environmental fluctuations and consequently affecting the TEC's cooling efficiency.

This model employs a disturbance-rejection tuning strategy to improve the PID controller's capacity to mitigate the effects of disturbances, such as abrupt fluctuations in sunlight intensity or temperature, on the TEC's temperature regulation. The PID controller for a TEC requires a balanced selection of gains (Kp, Ki, Kd) to achieve satisfactory performance across multiple characteristics, avoiding over-optimization of any single attribute. This method provides a more robust and reliable system that can consistently maintain temperature stability despite widely fluctuating inputs.

The input disturbance rejection-focused PID controller demonstrates superior adaptability to fluctuating solar irradiance and thermal loads. It enables faster Voltage and current compensation through the Buck-Boost converter, thereby maintaining more stable operating conditions for the TEC. This leads to lower electrical power consumption and improved system COP, especially under real-world conditions where PV output is variable. Despite introducing slightly higher current peaks, this tuning strategy proves more effective in enhancing overall energy efficiency and thermal stability.

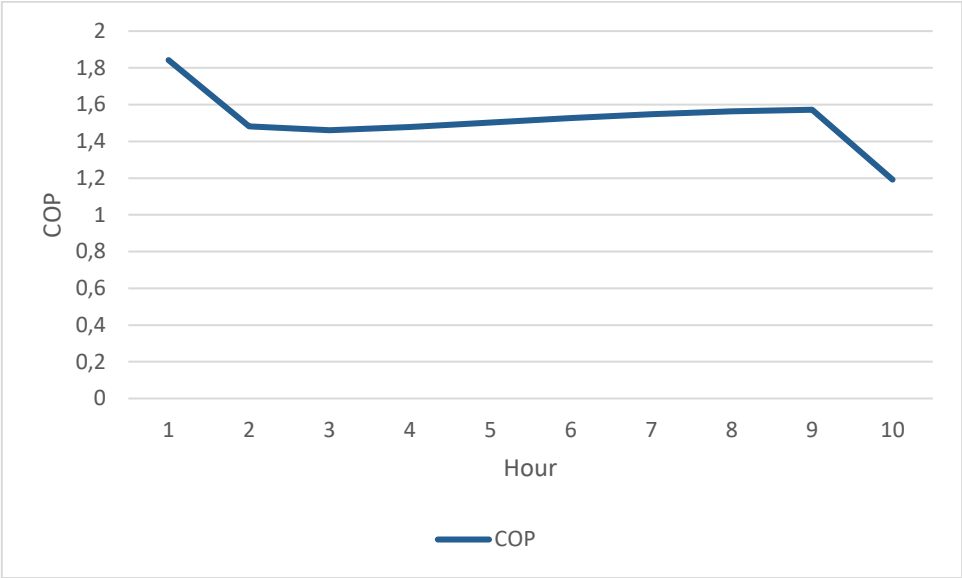

Figure 10 COP of the integrated PV-TEC system with PID-controlled DC-DC Buck-Boost converter, emphasizing current feedback for input disturbance rejection tuning

TECs can achieve maximum coefficients of performance under ideal operating conditions, and their operation is limited to the power required to achieve the setpoint, thereby optimizing efficiency and minimizing energy consumption. The use of a disturbance-rejecting PID controller mitigates fluctuations in solar PV input power, thereby ensuring optimal TEC operation in steady state. Implementation of enhanced voltage tracking optimizes TEC performance within its optimal coefficient-of-performance range. After integrating the PID controller, the system's performance improved significantly. By implementing a robust feedback system, the PID controller continuously monitored and modulated the TEC's temperature by dynamically adjusting the buck-boost converter's output current and voltage.

The Solar PV voltage and current output power the DC converter. Those DC boost converters actively convert the voltage, enabling the TEC to actively cool the Solar PV Panel and thereby increase its electrical power output; however, the TEC itself already consumes a small amount of power. There is a critical trade-off between power gained and the power consumed. For the cooling system to be effectively, economically, and practically viable, the increase in Solar PV power output, from its voltage mpp and current mpp, resulting from the cooling effect, must exceed the power required to activate the TEC. The slight rise could be due to the PID controller optimizing the TEC's operating voltage for the sustained maximum power output from the PV. By default, the TEC's COP is low (ranging from 0.4 to 0.7) (Ibikunle et al., 2022); therefore, a successful optimization strategy depends on achieving a higher COP to ensure a positive net power gain. If the TEC's COP is too low, the power consumed by the TEC may negate, or even exceed, the power gain, and we may conclude that the entire system is

counterproductive. There are two key factors of the method for having the TEC COP's higher, it depends highly on the temperature differences (ΔT), between the cold side (the Solar PV) and the hot side (the heat sink used to emit the heat to the ambient air) (Patel et al., 2016). The other points to provide suitable power to the TEC, which is supported by the DC-DC boost converter (Pal et al., 2024). The COP decreases dramatically as the required ΔT is increases. Therefore, a decrease in ΔT should increase TEC's COP. At the optimal operating point, lowering the backside temperature of the Solar PV to ambient temperature is considered a more manageable target, instantly maximizing the TEC's COP.

The graph in Figure 10 shows the TEC's sensitivity to the variation between ambient and operating temperatures (ΔT) and the dynamic control of the DC-DC boost converter. The consistent performance between Hours 4 and 9 shows an equilibrium between cooling needs and system efficiency, which is controlled by the duty cycle. The Duty Cycle D of the DC-DC boost converter is the primary control parameter that links the PV input power to the TEC's current and, ultimately, its COP. The power consumed by the TEC is drawn from the Solar PV, minus conversion losses. At low D approaching 0, there is no voltage step-up in the converter; therefore, the current output from the DC-DC Boost Converter (I_{out}) is also low, resulting in low cooling power (Q_C). Hence, the TEC consumes less power from the Solar PV system. And during the high D, when the Vout from the DC-DC Boost converter is significantly higher than Vin, Iout also increases instantly, resulting in higher cooling power and higher TEC power consumption. The controller in the DC-DC Boost Converter will adjust D to draw more power from the Solar PV. Apart from consuming the power from Solar PV, it tries to maximize the Net Power Gain, resulting from the subtraction of Solar PV-generated Power to DC-DC Boost Converter (conversion losses) and TEC Power consumption ($P_{PV_{gain}} - P_{DC-DC_{Boost_{Converter_{consumption}}}} - P_{TEC_{consumption}}$), by finding the optimal D.

From Figure 10, we can categorize that there are 3 (three) periods of controlling the D, (1) the morning hours from 1 to 2 hours, where the solar irradiance is low, then the Solar PV temperature is low, then the required (ΔT) for cooling is minimal. The system only needs a negligible Qc. Therefore, the controller set the D value to low to limit TEC power consumption; when Iout is high, P_{in_TEC} will be low. Since the cooling load is relatively low, the TEC operates far from its maximum ΔT, resulting in a high COP that gradually decreases. (2) the noon hours, from 2 to 9, where the solar irradiance is reaching its highest point, which instantly increases the Solar PV thermal load and causes the ΔT to increase. Solar irradiance is increasing rapidly and the PV cell temperature is rising fast, placing a sudden high thermal load on the TEC. Simultaneously, the PV power available to the TEC is also rapidly increasing. The initial drop suggests that the thermal load (heat to be removed) is increasing faster than the TEC's

efficiency can maintain, possibly due to the rapid temperature rise and the inertia of the system. The controller increases D to significantly boost Vout and Iout to the TEC, delivering the required Q_c. Given a substantial increase in Iout and a higher ΔT, the TEC's COP declines progressively. Therefore, a gradual decrease in the COP during peak sun hours is observed; the stable COP should be considered. The controller holds the D value to achieve the maximum net power, accepting a gradual COP drop as the necessary trade-off for maximizing Power gain from Solar PV. The stable curve confirms the thermal synergy between passive and active cooling along with the PID controller's success in rejecting the input disturbances (changing irradiance/temperature). (3) the late hours, from 9-10, where the irradiance drops along with the ambient temperature. To maintain a stable cooling effect or extract the maximum remaining power from the Solar PV, the controller will set D to a significantly high value. At high D values, the conduction and switching mechanisms are lost, as shown in Fig. 10, and the DC-DC boost converter's efficiency drops significantly. Furthermore, operating the TEC at very high current (Iout) beyond its optimal setting due to high D results in excessive Joule Heating within the TEC and a sharp drop in its COP.

Scenario 2: Scenario 1 with thermal collector and heat exchanger

High-performance, energy-efficient Solar PV is achieved by modeling a PV system integrated with a TEC and a DC-DC buck-boost converter, incorporating a PID controller with input disturbance-rejection-focused tuning, as seen in scenario 1 with the addition of a thermal collector and heat exchanger with air as the cooling fluid. The system effectively mitigates real-world challenges, including variations in solar irradiance (input disturbances) and excess heat from the solar photon reaction in the crystalline silicon, thereby ensuring stable power delivery through the DC-DC Buck-Boost Converter to the TEC, irrespective of environmental fluctuations and their consequent impact on the TEC's cooling efficiency.

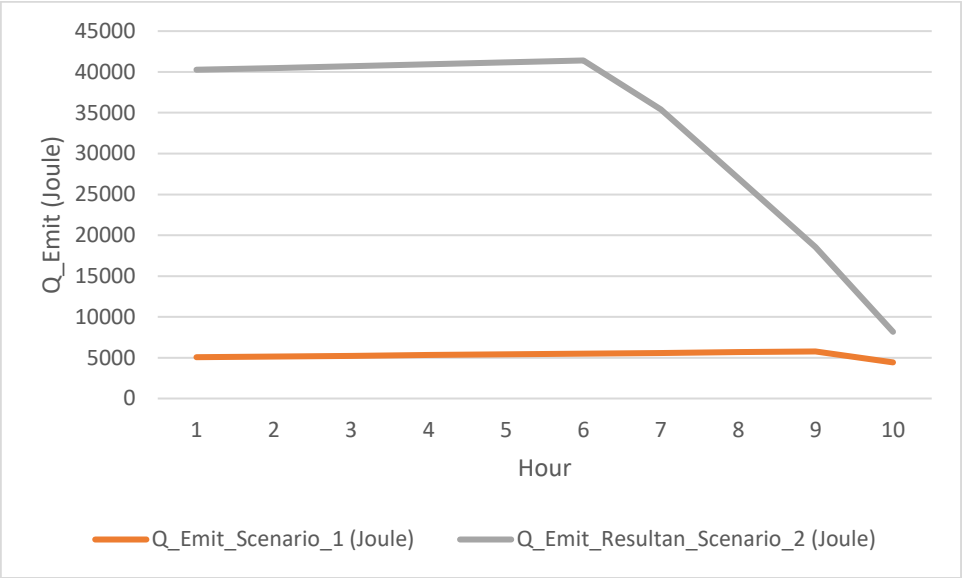

Figure 11 Q_Emit of the integrated PV/T-TEC system and PVTEC system

Q Emit in Figure 11 shows the heat removal, both by scenario 1 and scenario 2. Scenario 1 represents cooling by a TEC powered by a DC-DC boost converter, with only the TEC doing the cooling. Scenario 2 represents the PV/T air collector is the primary thermal management component, cooling using a PV/T collector with air as the cooling fluid, plus an additional TEC powered by a DC-DC boost converter (Hybrid PV/T-TEC cooling).

In the 1st scenario, the heat removal capacity is constrained by the power consumed by the TEC ($P_{in\ TEC}$) and power converstion losses due to the DC-DC Boost Converter and the TEC's low COP, whereas typically the COP is less than 1 or could reast up to 1.8 in the optimal condition (where the DC-DC Boost Converter is provided with PID controller to regulate the duty cycle). Although the TEC is well-suited for localized cooling, its overall heat-removal capacity is constrained relativeo the total excess heat generated by the Solar PV module (Ahmed et al., 2024). The system is designed to prioritize net electrical gain, resulting in lower Q emissions rather than simply maximizing heat removal.

In the 2nd scenario, the heat removal is significantly higher, approximately and considerably stable near 41000 joules during the peak sun hours (PSH) (from hours 1 ~ 6). During the PSH period, the Q emit remains nearly constant, indicating that the combined cooling system effectively removes the maximum excess heat generated by the Solar PV module during peak solar irradiance. The hybrid system maintaining a large, stable temperature differential between the hot PV surface and the ambient air. This large ΔT drives the high rate of heat transfer via natural convection (passive cooling). And beyond the PSH period (6-10), the Q emit drops sharply to approximately 8000 joules, exactly at hour 10. The drop is due to the rapid decrease in solar irradiance in the late afternoon, which causes a significant drop in

excess heat (heat generated by the reaction occurs in the Solar PV module). The reduced temperature differential significantly weakens the driving force for passive convection, causing the large QEmit contribution of the PV/T collector to diminish rapidly. Since there is less heat to remove, the total dissipated heat drops instantly.

In the summary, scenario 1 relies primarily on TEC active cooling, while scenario 2 mainly uses a thermal collector with air as the cooling fluid for passive cooling, combined with TEC for active cooling. The efficiency factor for scenario 1 is constrained by the TEC's power consumption and internal characteristics, which have a low COP. Scenario 2, which is considerably higher than scenario 1, is dominated by the PVT air collector, which provides high-thermal-mass-flow cooling. In scenario 2, the PV/T with air cooling is removing a massive amount of excess heat via natural convection, and the TEC is used as a secondary or booster to cool the solar PV back surface just enough to maximize electrical efficiency, effectively operating on the already-precooled panel. The PV/T air collector is significantly more efficient at transferring thermal energy than TEC, resulting in the much higher Q emitted observed in scenario 2.

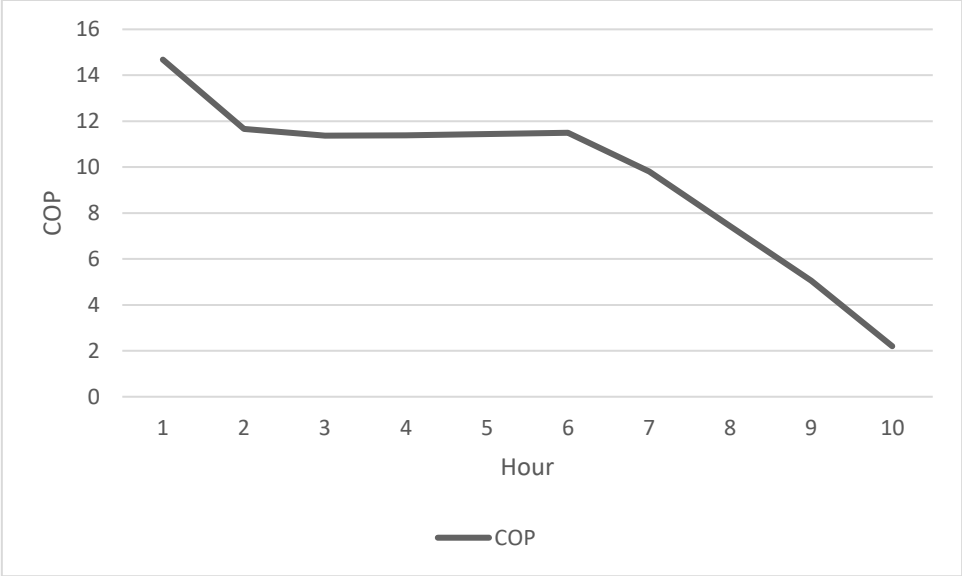

Figure 12 COP of the integrated PV/T-TEC system with PID-controlled DC-DC Buck-Boost converter, emphasizing current feedback for input disturbance rejection tuning

Figure 12's curve shows significant fluctuations in COP over 10 hours, potentially reflecting the operational cycle of the integrated Solar PV/T and TEC cooling system. Overall system functionality is determined by variations in solar irradiance and the associated thermal burden. Figure 12 presents the dynamic efficiency of the TEC as a function of solar load, subject to limitations imposed by the air-cooling system's thermal resistance. This curve underscores the complexity of TEC optimization: a high COP is achievable only at low thermal

loads, yet the system must maintain a lower, stable COP during peak hours to maximize the PV panel's overall electrical energy yield. From Figure 12, we can categorize that there are 3 (three) periods, (1) Morning ramp-up, where solar irradiance is increasing rapidly. The PV cell temperature is rising quickly, placing a sudden and increasing thermal load on the TEC. This rapid rise in the required ΔT (faster than the TEC's efficiency can adapt) causes the initial sharp drop in COP. (2) Midday Stability, where the COP stabilization indicates the system has achieved a thermal and electrical equilibrium. The high heat load is successfully balanced by the peak passive heat removal (Q_{Emit}), leading to a stable operating temperature and a stable COP. The PID controller is tuned for input disturbance rejection and dynamically adjusts the converter's duty cycle to ensure the TEC module maintains a stable and optimal power input despite the varying PV output. The fluctuations in solar irradiance and temperature cause the PV's MPP voltage and current to constantly change (input disturbances). The PID controller also prevents the COP from fluctuating wildly, confirming that the control strategy effectively maintains the TEC at its stable operating point to maximize the Net Electrical Power Gain during peak irradiance. (3) Afternoon decline, where solar irradiance is rapidly falling. As the input power available from the PV panel drops below the critical threshold required for the Boost Converter and TEC operation, the system reaches its electrical power constraints. The TEC can no longer operate efficiently, leading to the rapid and steep collapse of the COP.

Conclusions

The integrated Photovoltaic Thermal-Thermoelectric Cooler (PV/T-TEC) system offers a highly efficient solution to optimize PV panel energy yield by leveraging a synergistic hybrid cooling mechanism. Analysis of the Q_Emit curve reveals that the PV/T air collector is the primary thermal management component, with peak heat dissipation approximately 7.5 times that of the TEC-only configuration. The substantial passive heat-removal strategy successfully pre-cools the PV panel and stabilizes the TEC's hot-side temperature, which is essential for minimizing the required operational temperature differential ΔT. By virtue of this thermal synergy, the TEC can operate under highly favorable conditions, thereby addressing its inherent limitation of a low intrinsic COP.

The strategic thermal decoupling results in a system that achieves an exceptionally high calculated Effective System COP (peaking at 14.5), demonstrating the significant overall energy benefit of the combined approach. Diurnal COP curve analysis confirms that the system's efficiency is highly dynamic and constrained by solar irradiance, necessitating a midday compromise. During periods of maximum solar radiation, the DC-DC boost converter maintains the TEC at a stable operating point, thereby maximizing the Net Electrical Power Gain. The final steep drop in COP indicates that the system's operational period is limited by

electrical power constraints in the late afternoon, underscoring the need for optimal current control and system sizing to preserve the high-efficiency gains achieved through hybridization.

Based on the performance evaluation of the Integrated PV/T–TEC System with a PID enabled DC–DC Boost Converter with tuning strategies—input disturbance rejection focus, the following recommendations are proposed : (1) moving from the simulated environment to a physical prototype, including metal fin PV/T collector, the TEC module, the Buck-Boost converter, and the microcontroller implementing the PID control, and (2) introduce a battery energy storage system (BESS) into the model, which requires modifying the Buck-Boost DC-DC converter to manage charging/discharging cycles, including its protection system.

Acknowledgements

The author would like to express their gratitude and appreciation to Universitas Semarang for financing this study through the Penelitian Dosen Pemula (PDP) for an Indexed National/International Publication Universitas Semarang No.: 061/USM.H7.LPPM/L/2025.

References

Abdel-Khalik, S. I. (1976). Heat Removal Factor For A Flat-Plate Solar Collector With A Serpentine Tube. *Solar Energy*, *18*, 59–64.

Adeeb, J., Farhan, A., & Al-Salaymeh, A. (2019). Temperature effect on performance of different solar cell technologies. *Journal of Ecological Engineering*, *20*(5), 249–254. https://doi.org/10.12911/22998993/105543

Ahmed, Y. E., Maghami, M. R., Pasupuleti, J., Danook, S. H., & Basim Ismail, F. (2024). Overview of Recent Solar Photovoltaic Cooling System Approach. In *Technologies* (Vol. 12, Issue 9). Multidisciplinary Digital Publishing Institute (MDPI). https://doi.org/10.3390/technologies12090171

Ali Taher, N. A. H., & Al-Hamadani, A. A. F. (2024). Experimental Study and Performance Analysis of Thermoelectric Cooler Using Solar Photovoltaic Energy. *Applied Mechanics and Materials*, *922*, 135–144. https://doi.org/10.4028/p-Avq2c4

Amelia, A. R., Irwan, Y. M., Leow, W. Z., Irwanto, M., Safwati, I., & Zhafarina, M. (2016). Investigation of the effect temperature on photovoltaic (PV) panel output performance. *International Journal on Advanced Science, Engineering and Information Technology*, *6*(5), 682–688. https://doi.org/10.18517/ijaseit.6.5.938

Amrizal, Amrul, Winardi, W., Prasetyo, J., & Irsyad, M. (2022). Performance Analysis of PV/T-TEC Collector for The Tropical Climate Conditions of Indonesia. *Journal of*

Advanced Research in Fluid Mechanics and Thermal Sciences, *95*(2), 72–83. https://doi.org/10.37934/arfmts.95.2.7283

Balasaheb, S. M., Rubab, S. M., & Abbas, M. S. (2018). Improving The Efficiency of Solar Panel. *Indapur JournalNX-A Multidisciplinary Peer Reviewed Journal (ISSN*.

Bayendang, N. P., Kahn, M. T., & Balyan, V. (2021). Simplified Thermoelectric Cooler (TEC) with Heatsinks Modeling and Simulation using Matlab and Simulink based-on Dimensional Analysis. *AIUE Proceedings of the 2nd Energy and Human Habitat Conference 2021*, 1–8.

Bhattacharjee, S., & Saharia, B. J. (2014). A comparative study on converter topologies for maximum power point tracking application in photovoltaic generation. *Journal of Renewable and Sustainable Energy*, *6*(5). https://doi.org/10.1063/1.4900579

Corapsiz, M. R., & Kahveci, H. (2019). Voltage Control Strategy for DC-DC Buck-Boost Converter. *4th International Conference on Advances in Natural & Applied Sciences*, 436–446.

Dehra, H. (2018). Building-Integrated Thermoelectric Cooling-Photovoltaic (TEC-PV) Devices. In *Bringing Thermoelectricity into Reality*. InTech. https://doi.org/10.5772/intechopen.75472

Dimri, N., Tiwari, A., & Tiwari, G. N. (2018). Effect of thermoelectric cooler (TEC) integrated at the base of opaque photovoltaic (PV) module to enhance an overall electrical efficiency. *Solar Energy*, *166*, 159–170. https://doi.org/10.1016/j.solener.2018.03.030

Dokić, B. L., & Blanuša, B. (2015). PWM DC/DC Converters. In B. L. Dokić & B. Blanuša (Eds.), *Power Electronics: Converters and Regulators* (pp. 211–309). Springer International Publishing. https://doi.org/10.1007/978-3-319-09402-1_4

Esram, T., & Chapman, P. L. (2007). Comparison of photovoltaic array maximum power point tracking techniques. *IEEE Transactions on Energy Conversion*, *22*(2), 439–449. https://doi.org/10.1109/TEC.2006.874230

Faheem, M., Abu Bakr, M., Ali, M., Majeed, M. A., Haider, Z. M., & Khan, M. O. (2024). Evaluation of Efficiency Enhancement in Photovoltaic Panels via Integrated Thermoelectric Cooling and Power Generation. *Energies* , *17*(11). https://doi.org/10.3390/en17112590

Gholampour, M., & Ameri, M. (2016). Energy and exergy analyses of Photovoltaic/Thermal flat transpired collectors: Experimental and theoretical study. *Applied Energy*, *164*, 837–856. https://doi.org/10.1016/j.apenergy.2015.12.042

Ibikunle, R. A., Akintunde, M. A., Titiladunayo, I. F., & Adeleke, A. A. (2022). Estimation of coefficient of performance of thermoelectric cooler using a 30 W single-stage type.

International Review of Applied Sciences and Engineering, *13*(2), 124–132. https://doi.org/10.1556/1848.2021.00322

Kalogirou, S. A. (2009). Solar energy engineering: Processes and systems. In *Solar Energy Engineering: Processes and Systems*. https://doi.org/10.1016/B978-0-12-374501-9.X0001-5

Kazem, H. A. (2019). Evaluation and analysis of water-based photovoltaic/thermal (PV/T) system. *Case Studies in Thermal Engineering*, *13*. https://doi.org/10.1016/j.csite.2019.100401

Kotkondawar, A., Bhende, A., Khond, V., & Rayalu, S. (2021). Performance evaluation of PV-TEC coupling device for power production with improved hybrid nanocarbon based thermal material interface. *Energy Reports*, *7*, 6868–6875. https://doi.org/10.1016/j.egyr.2021.09.110

Laird Thermal Systems. (2022). *Thermoelectric Handbook*. Laird Thermal Systems. www.lairdthermal.com

Misha, S., Abdullah, A. L., Tamaldin, N., Rosli, M. A. M., & Sachit, F. A. (2020). Simulation CFD and experimental investigation of PVT water system under natural Malaysian weather conditions. *Energy Reports*, *6*, 28–44. https://doi.org/10.1016/j.egyr.2019.11.162

Molina-Santana, E., Gonzalez-Montañez, F., Liceaga-Castro, J. U., Jimenez-Mondragon, V. M., & Siller-Alcala, I. (2023). Modeling and Control of a DC-DC Buck–Boost Converter with Non-Linear Power Inductor Operating in Saturation Region Considering Electrical Losses. *Mathematics*, *11*(22). https://doi.org/10.3390/math11224617

Momoh, J. (2018). Converters and Inverters. In *Energy Processing and Smart Grid* (pp. 289–322). IEEE. https://doi.org/https://doi.org/10.1002/9781119521129.ch12

Mooko, G., & Kusakana, K. (2018). Prospective Use of Thermoelectric Device for PV Panel Cooling. *2018 Open Innovations Conference, OI 2018*, 68–72. https://doi.org/10.1109/OI.2018.8535716

Narkwatchara, P., Ratanatamskul, C., & Chandrachai, A. (2020). Effects of particulate matters and climate condition on photovoltaic system efficiency in tropical climate region. *Energy Reports*, *6*, 2577–2586. https://doi.org/10.1016/j.egyr.2020.09.016

Pal, S., Bhowmick, B., & Sinha, D. (2024, March). Review on DC-to-DC Boost Converter Control Topologies of Renewable Energy Applications. *Applied Computer Technology*.

Patel, J., Patel, M., Patel, J., & Modi, H. (2016). Improvement In The COP Of Thermoelectric Cooler. *International Journal of Scientific & Technology Research*, *5*(5), 5. www.ijstr.org

Pathiran, A. R. (2019). Improving the Regulatory Response of PID Controller Using Internal Model Control Principles. *International Journal of Control Science and Engineering*, *2019*(1), 9–14. https://doi.org/10.5923/j.control.20190901.02

Pratama Putra, I., Dyah Ekawati, E., Rizal Oktavian Wahyudi, M., Herdunan Christofer Zefanya, A., Zaidan Azhar, F., Wahyu Kushendranto, R., Nuzul Ramadhan, M., & Setyo Pambudi, W. (2023). Kendali Dc-Dc Converter Buck Boost Converter menggunakan PID Controller dengan Tuning Ziegler Nichols. *Prosiding Seminar Nasional Hasil Riset dan Pengabdia*, 1313–1319. https://snhrp.unipasby.ac.id/prosiding/index.php/snhrp/article/view/691/

Qadir, B. A., & Ati, M. (2024). Optimizing DC-DC Buck-Boost Converters with a PID Controller: Harnessing the Power of Silicon Carbide Technology. *International Conference on Engineering and Emerging Technologies, ICEET*, *2024*. https://doi.org/10.1109/ICEET65156.2024.10913738

Sesotyo, P. A., Muhamad Idris, L. O., Dwi Cahyono, T., & Sadewa, E. (2025). Evaluating of DC-DC Buck-Boost Converter implementation for Integrated Solar Photovoltaic and Thermoelectric Cooler System. *International Journal of Engineering Continuity*, *4*(1), 140–172. https://doi.org/10.58291/ijec.v4i1.372

Sesotyo, P. A., Sunaryo, S., Arifin, Z., & Basuki, P. (2022). Studying the Absorption Refrigeration System powered by Thermal Waste and Electricity Conversion from Photovoltaic. *Clean Energy and Smart Technology*, *1*(1), 15–22. https://doi.org/10.58641/cest.v1i1.3

Singh, P., & Ravindra, N. M. (2012). Temperature dependence of solar cell performance - An analysis. *Solar Energy Materials and Solar Cells*, *101*, 36–45. https://doi.org/10.1016/j.solmat.2012.02.019

Soheli, S. N., Sarowar, G., Hoque, Md. A., & Hasan, M. S. (2018). Design and Analysis of a DC -DC Buck Boost Converter to Achieve High Efficiency and Low Voltage Gain by using Buck Boost Topology into Buck Topology. *2018 International Conference on Advancement in Electrical and Electronic Engineering (ICAEEE)*, 1–4.

Talal, M. R., Ismaeel, A. A., & Kareem, I. S. (2024). A Review of the Existing Advance of Photovoltaic Thermal Air Collector: Drawbacks and Future Development. *Journal of Renewable Energy and Environment*, *11*(4), 165–204. https://doi.org/10.30501/jree.2024.466186.1988

Togun, H., Basem, A., Kadhum, A. A. H., Abed, A. M., Biswas, N., Rashid, F. L., Lawag, R. A., Ali, H. M., Mohammed, H. I., & Mandal, D. K. (2025). Advancing photovoltaic thermal (PV/T) systems: Innovative cooling technique, thermal management, and future prospects. In *Solar Energy* (Vol. 291). Elsevier Ltd. https://doi.org/10.1016/j.solener.2025.113402

Toumi, D., Benattous, D., Ibrahim, A., Abdul-Ghaffar, H. I., Obukhov, S., Aboelsaud, R., Labbi, Y., & Diab, A. A. Z. (2021). Optimal design and analysis of DC–DC converter with maximum power controller for stand-alone PV system. *Energy Reports*, *7*, 4951–4960. https://doi.org/10.1016/j.egyr.2021.07.040

Tsai, H. L., & Lin, J. M. (2010). Model building and simulation of thermoelectric module using Matlab/Simulink. *Journal of Electronic Materials*, *39*(9), 2105–2111. https://doi.org/10.1007/s11664-009-0994-x

Twaha, S., Zhu, J., Yan, Y., Li, B., & Huang, K. (2017). Performance analysis of thermoelectric generator using dc-dc converter with incremental conductance based maximum power point tracking. *Energy for Sustainable Development*, *37*, 86–98. https://doi.org/10.1016/j.esd.2017.01.003

Wu, Y. Y., Wu, S. Y., & Xiao, L. (2015). Performance analysis of photovoltaic-thermoelectric hybrid system with and without glass cover. *Energy Conversion and Management*, *93*, 151–159. https://doi.org/10.1016/j.enconman.2015.01.013